Effect of Functional Groups on Microporous Polymer Based Resisitance Switching Memory Device

Yaru Song,[‡ab] Jie Liu,[‡ab] Wanhui Li,[ab] Lei Liu,[ab] Ling Yang[c], Shengbin Lei,[*ab] and Wenping Hu[a]

a. Tianjin Key Laboratory of Molecular Optoelectronic Science, Tianjin University, Tianjin 300072, P. R. China

b. Department of Chemistry, School of Science & Collaborative Innovation Center of Chemical Science and Engineering (Tianjin), Tianjin University, Tianjin 300072, P. R. China

*Email: shengbin.lei@tju.edu.cn

Electronic Supplementary Information

Experimental details

Synthesis of microporous covalent organic polymer ($MP_{TPA+TAPB}$ and $MP_{OTPA+TAPB}$):

All chemicals were used without further purification. The experimental process is as follows: First, 20 mL deionized water was prepared in a φ7 cm bottle. Then, 1.4 mg (0.004 mmol) of 1,3,5-tris(4-aminophenyl)-benzene (TAPB) powder and 8 mg (0.006 mmol) of terephthalaldehyde (TPA) were dissolved in 2mL DMF and then 40 μL of acetic acid were added. 50, 100, 200, 300 μL of this mixture solution were diluted by 300 μL chlorobenzol, and then carefully dropped on the surface of the deionized water respectively. The microporous polymer films were finally obtained at the solution/air interface after the bottle was set in room temperature for 48 h. In the above-mentioned preparation process, the amount of the monomer mixture dropped on the water surface determines the thickness of the MP films. The thickness of the MP films gradually increases with the increase of the volume of the monomer solution dropped on the water surface. By controlling the volume solution dropped on the water surface, the thickness of the MP film can be effectively controlled in the range from 15 to 80 nm.

Device fabrication:

The Ag/MP/ITO devices were fabricated on the indium-tin-oxide (ITO) glass substrate. The substrates (1 cm×1 cm) were sequentially pre-cleaned with methylbenzene, acetone, ethanol, isopropanol and deionized water. The synthesized MP films were first transferred onto the surface of water and DMF to remove unreacted precursors. Then, the active organic film was transferred onto the ITO glass substrate. Finally, the Ag top electrode (with thickness of 50 nm) was deposited through a shadow mask. The area of electrode is 6.8×10^{-3} mm^2. The memory characteristics of devices were measured using a probe station at room temperature.

The process of collecting BET samples:

In order to collect the samples for BET measurement, we prepared the film samples in 16 identical weighing bottles each time. And we first transfer a part of MP films to confirm the quality of MP films by optical microscopy and AFM method, and then collect the same films. Washing was carried out after transfer the MP films from

water-air interface to DMF solvent to remove the monomer and oligomer. The samples were then dried in vacuum at 60 °C over night to completely remove the solvent. These collection processes were repeated about 25 times and finally 10 mg ($MP_{TPA+TAPB}$) and 8 mg ($MP_{OTPA+TAPB}$) samples were collected, respectively.

Characterization

Optical microscope images were taken using the Nikon ECLIPSE Ci-POL polarized optical microscope with a blue filter. SEM images of the samples were taken using the Hitachi SEM SU8010 Field Emission Scanning Electron Microscope (FESEM). The AFM image was obtained using a Bruker Dimension Icon AFM instrument with tapping mode. UV–vis absorption spectra were carried out at room temperature with a SHZMADZU UV-3600 Plus spectrophotometer. The Attenuated Total Reflectance FTIR (ATR FTIR) spectra of $MP_{TPA+TAPB}$ and $MP_{OTPA+TAPB}$ film were obtained using the Bruker vertex 70. Samples for transmission electron microscopy (TEM) examination were transferred to a holey copper TEM grid (i.e. coated with carbon film) and all high-resolution TEM and SAED images were obtained using a Tecnai G2 F20 S-TWIN. XPS measurements were carried on the Thermo Fisher Scientific ESCALAB 250Xi. The BET (Brunauer-Emmett-Teller) and pore size properties were measured by BELSOPR-mini II. The *I–V* measurements were performed using a micromanipulator 6150 probe station connected to a Keithley 4200-SCS. All of the electrical measurements were carried out in an ambient air environment.

The electrochemical properties of $MP_{TPA+TAPB}$ and $MP_{OTPA+TAPB}$ films were investigated by cyclic voltammograms (CVs) to determine the HOMO and LUMO energy levels. The measurement was carried out in acetonitrile using Au as the working electrode, Ag/AgCl as the reference electrode and platinum wire as the counter electrode. According to the CV of Figure S12b, both films showed irreversible oxidation behavior, and for the $MP_{TPA+TAPB}$ and $MP_{OTPA+TAPB}$ films, the oxidation peaks appear at 1.49 and 1.30 eV, respectively. The HOMO energy levels can be calculated from the onset oxidation potential with reference to ferrocene (4.8 eV) by the following equation：

$HOMO(eV)=-[E_{ox(onset)vsAg/AgCl}+4.8-E_{1/2(ferrocene)}]$,[1,2] whereas the LUMO energy levels can be determined based on the HOMO and the optical bandgap. The HOMO and LUMO values were determined to be -5.85 eV (or -5.66 eV) and -3.26 eV (or -3.25 eV) for a $MP_{TPA+TAPB}$ (or $MP_{OTPA+TAPB}$) film.

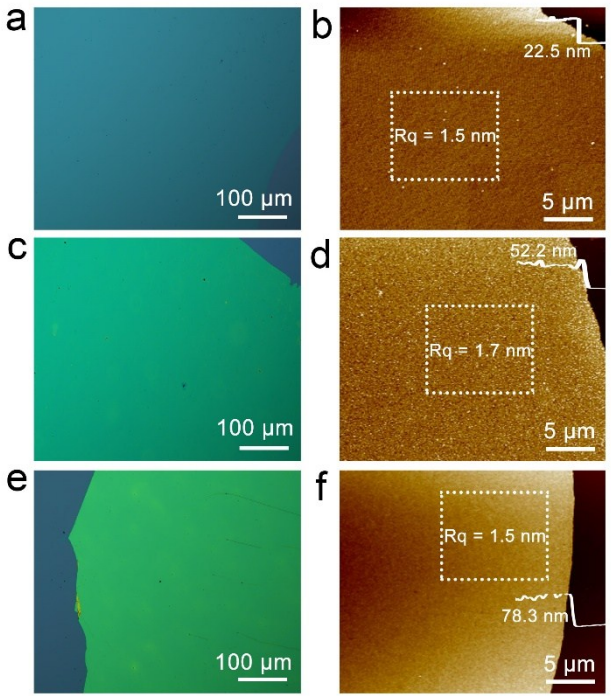

Figure S1. a. Optical microscopy of $MP_{TPA+TAPB}$ (about 22.5 nm). **b.** AFM image of $MP_{TPA+TAPB}$ (about 22.5 nm). **c.** Optical microscopy of $MP_{TPA+TAPB}$ (about 52.2 nm). **d.** AFM image of $MP_{TPA+TAPB}$ (about 52.2 nm). **e.** Optical microscopy of $MP_{TPA+TAPB}$ (about 78.3 nm). **f.** AFM image of $MP_{TPA+TAPB}$ (about 78.3 nm).

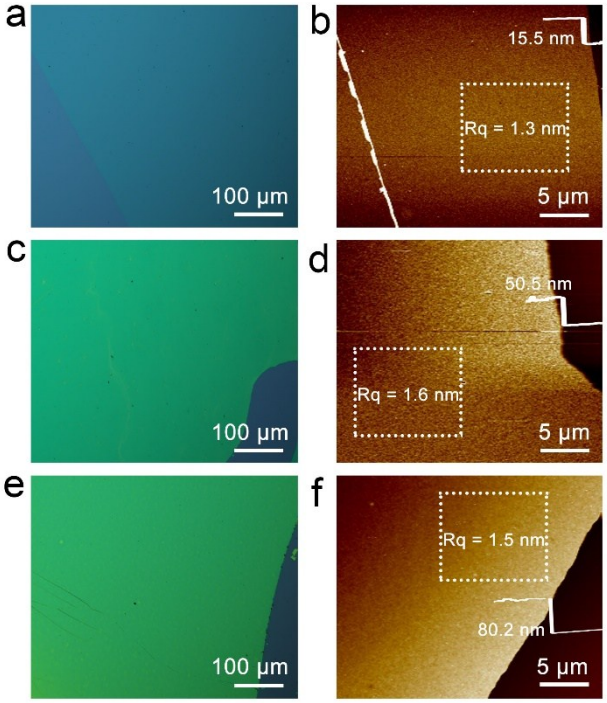

Figure S2. a. Optical microscopy of $MP_{OTPA+TAPB}$ (about 15.5 nm). **b.** AFM image of $MP_{OTPA+TAPB}$ (about 15.5 nm). **c.** Optical microscopy of $MP_{OTPA+TAPB}$ (about 50.5 nm). **d.** AFM image of $MP_{OTPA+TAPB}$ (about 50.5 nm). **e.** Optical microscopy of $MP_{OTPA+TAPB}$ (about 80.2 nm). **f.** AFM image of $MP_{OTPA+TAPB}$ (about 80.2 nm).

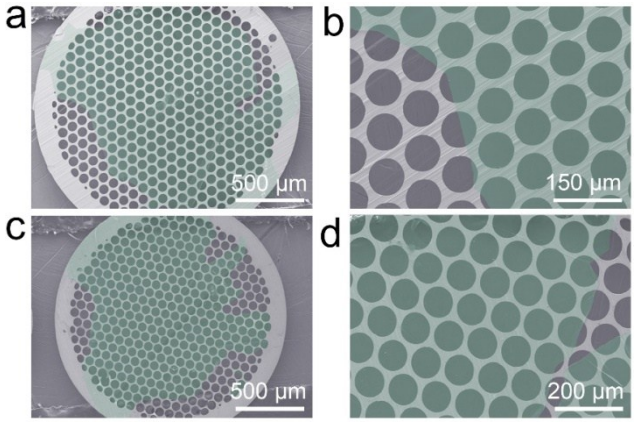

Figure S3. a. SEM image of $MP_{TPA+TAPB}$ with the thickness of about 22.5 nm on a bare copper mesh (large range). **b.** SEM image of $MP_{TPA+TAPB}$ with the thickness of about 22.5 nm on a bare copper mesh (small range). **c.** SEM image of $MP_{OTPA+TAPB}$ with the thickness of about 15.5 nm on a bare copper mesh (large range). **d.** SEM image of $MP_{OTPA+TAPB}$ with the thickness of about 15.5 nm on a bare copper mesh (small range).

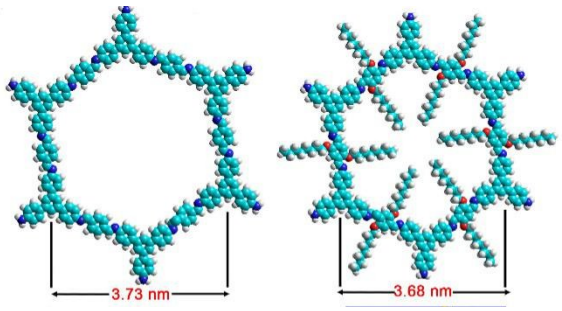

Figure S4. Optimized structure of $MP_{TPA+TAPB}$ (left) and the $MP_{OTPA+TAPB}$ (right).

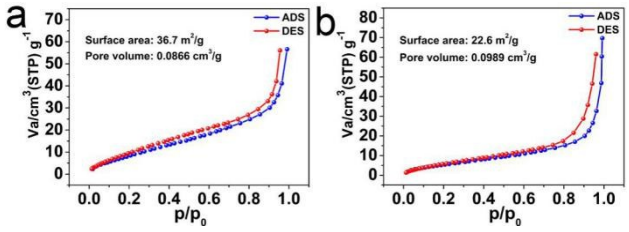

Figure S5. a. Nitrogen adsorption (blue ball) and desorption (red ball) isotherm profiles of $MP_{TPA+TAPB}$ at 77 K. **b.** Nitrogen adsorption (blue ball) and desorption (red ball) isotherm profiles of $MP_{OTPA+TAPB}$ at 77 K.

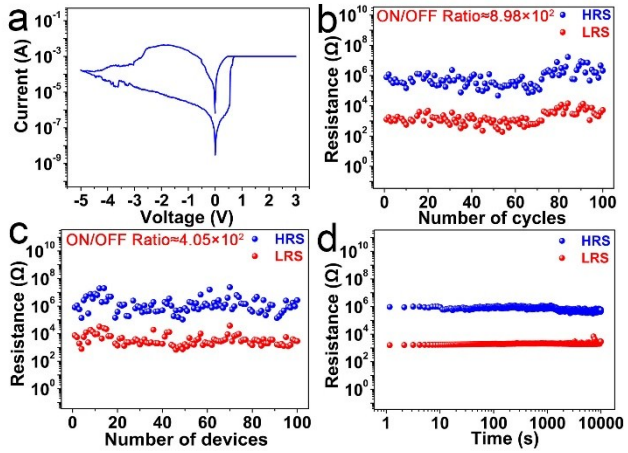

Figure S6. a. *I-V* characteristics of the Ag/$MP_{TPA+TAPB}$/ITO device (about 22.5 nm, V_{SET} ~0.54 V). **b.** Distribution of the HRS resistance and LRS resistance for Ag/$MP_{TPA+TAPB}$/ITO device under 100-time continuous switching cycles (about 22.5 nm) (read at -0.1 V). **c.** The device-to-device distributions of HRS resistance and LRS resistance for Ag/$MP_{TPA+TAPB}$/ITO devices (about 15-20 nm) (read at -0.1 V). **d.** Retention time of the Ag/$MP_{TPA+TAPB}$/ITO device (about 22.5 nm) in the "ON" and "OFF" states at reading voltage of 0.1 V. The tests on more than 100 devices produce a high success rate of 90%.

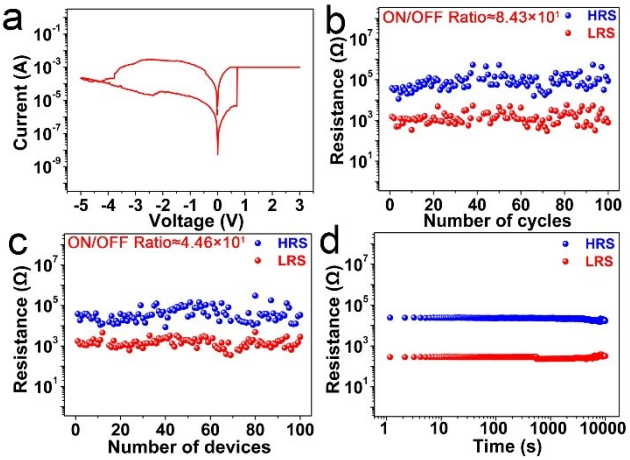

Figure S7. a. *I-V* characteristics of the Ag/$MP_{OTPA+TAPB}$/ITO device (about 15.5 nm, V_{SET} ~0.70 V). **b.** Distribution of the HRS resistance and LRS resistance for Ag/$MP_{OTPA+TAPB}$/ITO device under 100-time continuous switching cycles (about 15.5 nm) (read at -0.1 V). **c.** The device-to-device distributions of HRS resistance and LRS resistance for Ag/$MP_{OTPA+TAPB}$/ITO devices (about 15-20 nm) (read at -0.1 V). **d.** Retention time of the Ag/$MP_{OTPA+TAPB}$/ITO device (about 15.5 nm) in the "ON" and "OFF" states at reading voltage of 0.1V. The tests on more than 100 devices produce a high success rate of 92%.

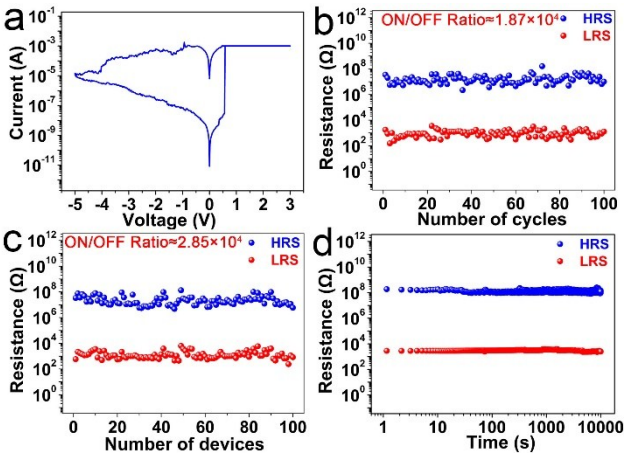

Figure S8. a. *I-V* characteristics of the Ag/$MP_{TPA+TAPB}$/ITO device (about 78.3 nm, V_{SET} ~0.56 V). **b.** Distribution of the HRS resistance and LRS resistance for Ag/$MP_{TPA+TAPB}$/ITO device under 100-time continuous switching cycles (about 78.3 nm) (read at -0.1 V). **c.** The device-to-device distributions of HRS resistance and LRS resistance for Ag/$MP_{TPA+TAPB}$/ITO devices (about 70-80 nm) (read at -0.1 V). **d.** Retention time of the Ag/$MP_{TPA+TAPB}$/ITO device (about 78.3 nm) in the "ON" and "OFF" states at reading voltage of 0.1 V. The tests on more than 100 devices produce a high success rate of 97%.

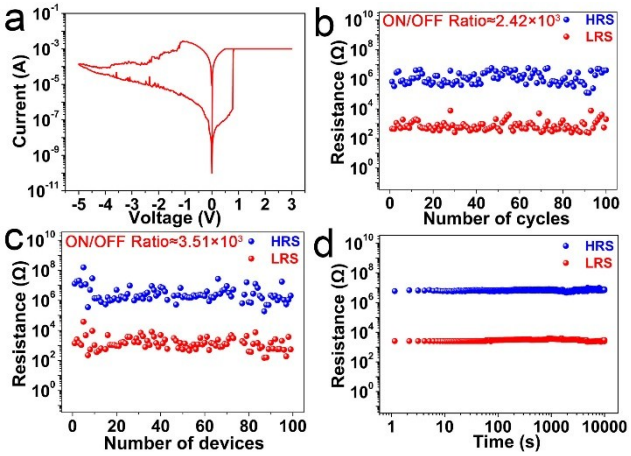

Figure S9. a. *I-V* characteristics of the Ag/$MP_{OTPA+TAPB}$/ITO device (about 80.2 nm, V_{SET} ~0.80 V). **b.** Distribution of the HRS resistance and LRS resistance for Ag/$MP_{OTPA+TAPB}$/ITO device under 100-time continuous switching cycles (about 80.2 nm) (read at -0.1 V). **c.** The device-to-device distributions of HRS resistance and LRS resistance for Ag/$MP_{OTPA+TAPB}$/ITO devices (about 70-80 nm) (read at -0.1 V). **d.** Retention time of the Ag/$MP_{OTPA+TAPB}$/ITO device (about 80.2 nm) in the "ON" and "OFF" states at reading voltage of 0.1 V. The tests on more than 100 devices produce a high success rate of 96%.

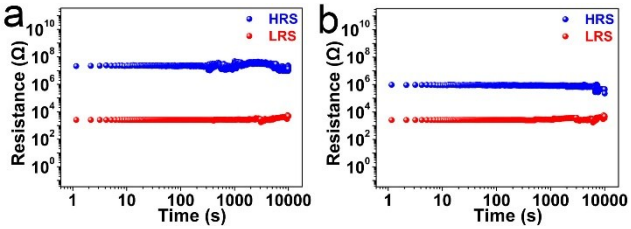

Figure S10. a. Retention time of the Ag/$MP_{TPA+TAPB}$/ITO devices (about 52.2 nm) in the "ON" and "OFF" states at reading voltage of 0.1 V. **b.** Retention time of the Ag/$MP_{OTPA+TAPB}$/ITO

devices (about 50.5 nm) in the "ON" and "OFF" states at reading voltage of 0.1 V.

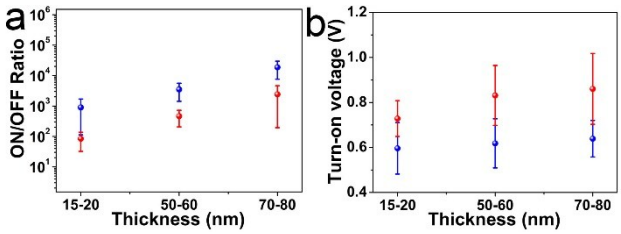

Figure S11. a. The error map of the on/off ratios for Ag/MP/ITO devices under 100-time continuous switching cycles with different thicknesses (read at -0.1 V). **b.** The error map of the turn-on voltages for Ag/MP/ITO devices under 100-time continuous switching cycles with different thicknesses.

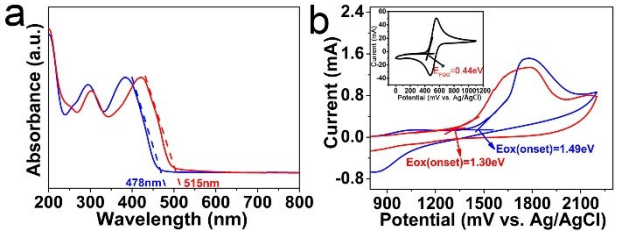

Figure S12. a. UV-Vis spectra of $MP_{TPA+TAPB}$ film (blue) and $MP_{OTPA+TAPB}$ film (red). **b.** CV curve of $MP_{TPA+TAPB}$ film (blue) and $MP_{OTPA+TAPB}$ film (red) on the Au electrode in 0.1 M tetrabutylammonium hexafluorophosphate ($n\text{-}Bu_4NPF_6$)/CH_3CN solution with Ag/AgCl as the reference electrode and Pt wire as the counter electrode. The inset shows the CV curve of the ferrocene standard, swept in the same conditions as for the two films. $E_{1/2}$(ferrocene) was measured to be 0.44 eV vs. Ag/AgCl in CH_3CN. The concentration of ferrocene in CH_3CN is 0.1 mol/L. $E_{eg}=h\nu=hC/\lambda=1240/\lambda=1240/478$ (1240/515) =2.59 (2.41) eV; $E_{HOMO}=-[E_{ox}(onset)$*vs*$Ag/AgCl+4.8-E_{1/2}(ferrocene)]$; $E_{LUMO}=E_{eg}+E_{HOMO}$.

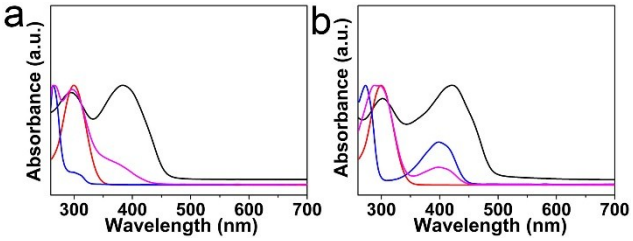

Figure S13. a. UV-Vis spectra of $MP_{TPA+TAPB}$ film (black), TAPB (red) and TPA (blue) in DMF solution and mixture solution of TAPB and TPA (pink). **b.** UV-Vis spectra of $MP_{OTPA+TAPB}$ film (black), TAPB (red) and OTPA (blue) in DMF solution and mixture solution of TAPB and OTPA (pink).

Table S1 The device-to-device distributions of HRS resistance and LRS resistance for Ag/MP/ITO devices with different thicknesses (read at -0.1 V).

	15-20nm $MP_{TPA+TAPB}$	15-20nm $MP_{OTPA+TAPB}$	50-60nm $MP_{TPA+TAPB}$	50-60nm $MP_{OTPA+TAPB}$	70-80nm $MP_{TPA+TAPB}$	70-80nm $MP_{OTPA+TAPB}$
HRS average (Ω)	2.05E+06	8.18E+04	6.26E+06	7.76E+05	5.06E+07	4.77E+06
LRS average (Ω)	5.28E+03	2.07E+03	2.21E+03	2.25E+03	2.23E+03	2.08E+03
ON/OFF ratio average	4.05E+02	4.46E+01	3.72E+03	4.54E+02	2.85E+04	3.51E+03

HRS relative standard deviation	176.48%	95.70%	68.82%	86.04%	99.80%	110.10%
LRS relative standard deviation	133.81%	47.96%	56.92%	84.05%	81.35%	90.22%
ON/OFF ratio relative standard deviation	58.32%	55.19%	56.56%	54.59%	61.10%	70.24%

Table S2 The device-to-device distributions of turn-on voltage for Ag/MP/ITO devices with different thicknesses.

	15-20nm $MP_{TPA+TAPB}$	15-20nm $MP_{OTPA+TAPB}$	50-60nm $MP_{TPA+TAPB}$	50-60nm $MP_{OTPA+TAPB}$	70-80nm $MP_{TPA+TAPB}$	70-80nm $MP_{OTPA+TAPB}$
Turn-on voltage average (V)	0.5314	0.7348	0.5910	0.8943	0.6054	0.9018
Turn-on voltage relative standard deviation	18.03%	11.19%	18.27%	17.63%	8.94%	18.88%

Table S3 Distribution of the HRS resistance and LRS resistance for Ag/MP/ITO devices under 100-time continuous switching cycles with different thicknesses (read at -0.1 V).

	15-20nm $MP_{TPA+TAPB}$	15-20nm $MP_{OTPA+TAPB}$	50-60nm $MP_{TPA+TAPB}$	50-60nm $MP_{OTPA+TAPB}$	70-80nm $MP_{TPA+TAPB}$	70-80nm $MP_{OTPA+TAPB}$
HRS average (Ω)	1.10E+06	1.11E+05	3.68E+06	5.53E+05	1.86E+07	1.79E+06
LRS average (Ω)	1.22E+03	1.43E+03	1.11E+03	1.12E+03	1.01E+03	1.01E+03
ON/OFF ratio average	8.98E+02	8.43E+01	3.50E+03	4.57E+02	1.87E+04	2.42E+03
HRS relative standard deviation	198.56%	74.97%	69.71%	99.28%	98.75%	85.61%
LRS relative standard deviation	96.98%	52.75%	64.03%	60.43%	58.86%	122.16%
ON/OFF ratio relative standard deviation	87.50%	61.85%	60.16%	55.39%	59.28%	91.97%

Table S4 Distribution of the turn-on voltage for Ag/MP/ITO devices under 100-time continuous switching cycles with different thicknesses.

	15-20nm $MP_{TPA+TAPB}$	15-20nm $MP_{OTPA+TAPB}$	50-60nm $MP_{TPA+TAPB}$	50-60nm $MP_{OTPA+TAPB}$	70-80nm $MP_{TPA+TAPB}$	70-80nm $MP_{OTPA+TAPB}$
Turn-on voltage average (V)	0.5960	0.7282	0.6182	0.8312	0.6388	0.8602
Turn-on voltage relative standard deviation	11.43%	7.95%	10.91%	13.31%	8.11%	15.73%

Table S5 Comparison of the chemical structure, BET data, ON/OFF ratio, and turn-on voltage in this work with the $2DP_{BTA+PDA}$ thin films in Reference 23.

	Chemical structure	BET data	ON/OFF ratio	Turn-on voltage
Reference 23	Benzene-1,3,5-tricarbaldehyde (BTA); p-phenylenediamine (PDA)	$2DP_{BTA+PDA}$ BET surface area: 74.4 m^2/g Pore volume: 8.82×10^{-2} cm^3/g Pore size: 1.41 nm	10^2 to 10^5	0.90±0.15 V
This work	1,3,5-tris(4-aminophenyl)-benzene (TAPB); Terephthalaldehyde (TPA); 2,5-dioctyloxyterephthalaldehyde (OTPA)	$MP_{TPA+TAPB}$: BET surface area: 36.7 m^2/g Pore volume: 8.66×10^{-2} cm^3/g Pore size: 5.71 nm $MP_{OTPA+TAPB}$: BET surface area: 22.6 m^2/g Pore volume: 9.89×10^{-2} cm^3/g Pore size: 2.85 nm	$MP_{TPA+TAPB}$: 4.05×10^2-2.85×10^4 $MP_{OTPA+TAPB}$: 4.46×10^1-3.51×10^3	$MP_{TPA+TAPB}$: 0.53±0.20-0.61±0.20 V $MP_{OTPA+TAPB}$: 0.73±0.20-0.90±0.20 V

Table S6 Comparison of the properties of devices in this work with devices based on other polymer/organic thin films.

Material type	Memory type	Turn-on voltage	ON/OFF ratio	Reference
Polyimides	DRAM	About 3.2 V	10^5	26
	WORM	About 1.8 V	10^5	27
	WORM and DRAM	1.5 to 3 V	10^7;10^8; 10^6	28
Polymers Containing Azobenzene Groups	WORM	Below −2 V	10^5 to 10^6	29
Polymers Containing Carbazole Groups	WORM	About -1.7 V	10^6	30
	WORM	−2.0 to −2.8 V	10^5	31
Polymers Containing Metal Complexes	WORM	About 2.5 V	10^6	32
Organic Small Molecules	WORM	About -3 V	$10^{3.93}$	33
2D polymers	Flash	0.90±0.15 V	10^2 to 10^5	21
This work	Flash	0.5 to 0.9 V	10 to 10^4	

References

1. J. L. Bredas, R. Silbey, D. S. Boudreaux, R. R. Chance, *J. Am. Chem. Soc*., 1983, **105(22)**, 6555-6559.

2. Y. Z. Lee, X. Chen, S. A. Chen, P. K. Wei, W. S. Fann, *J. Am. Chem. Soc*., 2001, **123**, 2296-2307.